IL NUOVO CIMENTO Vol. 36 C, N. 1 Gennaio-Febbraio 2013
DOI 10.1393/ncc/i2013-11418-5

Colloquia: IFAE 2012

Highlights from the ARGO-YBJ experiment

B. D'Ettorre Piazzoli for the ARGO-YBJ Collaboration

Dipartimento di Fisica, Universitá "Federico II", Napoli and INFN Sezione di Napoli Napoli, Italy

ricevuto il 31 Agosto 2012

Summary. — The ARGO-YBJ experiment is in stable data taking since November 2007 at the YangBaJing Cosmic Ray Laboratory (Tibet, P.R. China, 4300 m a.s.l., 606 g/cm^2). The results from the first 3.5 years of operation are reviewed.

PACS 96.50.S- – Cosmic rays.
PACS 96.50.sd – Extensive air showers.

1. – Introduction

The ARGO-YBJ detector, hosted in the YangBaJing Cosmic Ray Laboratory (Tibet, P.R. China, 4300 m a.s.l., 606 g/cm^2) is in stable data taking since November 2007. Location and detector features make ARGO-YBJ capable of investigating a wide range of fundamental issues in Cosmic Ray at a relatively low-energy threshold. In the following sections, after a description of the detector and its performance, the main results achieved after about 3.5 years of stable data taking are reviewed.

2. – The ARGO-YBJ experiment

The ARGO-YBJ experiment is currently the only air shower array with a dense sampling active area operated at high altitude, with the aim of studying the cosmic radiation at an energy threshold of a few hundred GeV. The large field of view (~ 2 sr) and the high duty cycle ($\geq 85\%$) allow a continuous monitoring of the sky in the declination band from $-10°$ to $70°$.

The detector is composed of a central carpet $\sim 74 \times 78\,\mathrm{m}^2$ large, made of a single layer of Resistive Plate Chambers (RPCs) with $\sim 93\%$ of active area, enclosed by a guard ring partially ($\sim 20\%$) instrumented with RPCs up to $\sim 100 \times 110\,\mathrm{m}^2$. Each chamber is read by 80 external strips of $6.75 \times 61.8\,\mathrm{cm}^2$ (the spatial pixels), logically organized in 10 independent pads of $55.6 \times 61.8\,\mathrm{cm}^2$ which represent the time pixels of the detector. The read-out of 18360 pads and 146880 strips is the digital output of the detector [1]. In addition, in order to extend the dynamical range up to PeV

energies, each chamber is equipped with two large size pads ($139 \times 123\,\mathrm{cm}^2$) to collect the total charge developed by the particles hitting the detector. The high granularity of the detector readout allows a detailed reconstruction of the space-time profile of the shower front and of the charge distribution around the core. ARGO-YBJ operates in two independent acquisition modes: the *shower mode* and the *scaler mode*. In shower mode, for each event the location and timing of every detected particle is recorded, allowing the reconstruction of the lateral distribution and the arrival direction. In scaler mode the total counts on each cluster are measured every 0.5 s in order to lower the energy threshold down to $\sim 1\,\mathrm{GeV}$. In shower mode a simple, yet powerful, electronic logic has been implemented to build an inclusive trigger. The whole system is in stable data taking since November 2007, with the trigger condition $N_{pad} \geq 20$, that is requiring at least 20 fired pads on the central carpet. The trigger rate is $\sim 3.5\,\mathrm{kHz}$ with a dead time of 4%. All the results presented in this paper have been obtained by analysing the data collected with the digital readout.

2˙1. *Detector performance.* – The performance of the detector (angular resolution, absolute pointing accuracy and the energy scale) and operation stability are continuously monitored by observing the Moon shadow, *i.e.*, the deficit of cosmic rays (CR) detected in its direction. With all data up to November 2010 we observed the CR Moon shadowing effect with a significance of about 70 s.d. The measured angular resolution is better than 0.5° for CR-induced showers with energies $E > 5\,\mathrm{TeV}$, in excellent agreement with the MC evaluation. With the same simulation codes we find that the angular resolution for *gamma*-rays is smaller by about 30–40%, depending on the multiplicity, due to the better defined time profile of the showers. The overall absolute pointing accuracy is $\sim 0.2°$.

The relation between the observed strip multiplicity and the CR primary energy is fixed with an uncertainty less than 13% in the energy range 1–30 TeV/Z [2].

3. – Gamma-Ray Astronomy

With about 3.5 years of data we observed 5 sources with a significance greater than 5 s.d.: Crab Nebula, Mrk421, Mrk501, MGRO J1908+06 and MGRO J2031+41. The analysis of Mrk501 is in progress. Details on the analysis procedure (*e.g.*, data selection, background evaluation) are given in [3, 4].

3˙1. *Crab Nebula and sky survey.* – We observed the Crab signal with a significance of 17 s.d. in about 1200 days, without any event selection to reject hadron induced showers.

The observed flux is consistent with a steady emission, and the observed differential energy spectrum in the 0.3–30 TeV range is $\mathrm{d}N/\mathrm{d}E = (3.0 \pm 0.3_{\mathrm{stat}}) \cdot 10^{-11} \cdot (E/1\,\mathrm{TeV})^{-2.57\pm0.09_{\mathrm{stat}}}\,\mathrm{cm}^{-2}\,\mathrm{s}^{-1}\,\mathrm{TeV}^{-1}$ in agreement with other measurements [5]. From these data we obtain that after 3.5 years of data taking the integrated sensitivity of ARGO-YBJ, without any rejection of the hadronic background, is of 0.3 Crab units. The map of the Northern hemisphere ($-10° < \delta < 70°$, δ = declination) will be released by the end of 2013 after data reprocessing with an improved reconstruction and applying the selection criteria for hadron-induced shower rejection. A sensitivity ≤ 0.2 Crab units at TeV energies is expected.

3˙2. *The blazar Markarian 421.* – Mrk421 is one of the brightest blazars and the closest to us ($z = 0.031$), characterized by a strong broadband flaring activity. The Mrk421 high variability makes the long-term multiwavelength observation very important to constrain the emission mechanisms models.

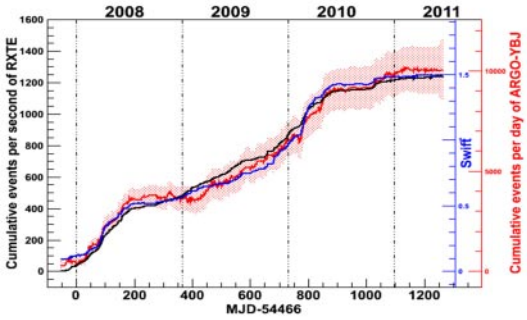

Fig. 1. – Cumulative light curve from Mrk421 measured by ARGO-YBJ (red curve) compared with RXTE/ASM (black curve) and Swfit (blue curve) X-ray data. The shaded red region indicates the corresponding 1σ statistical error.

ARGO-YBJ detected different TeV flares in correlation with X-ray observations, as can be seen in fig. 1 where the ARGO-YBJ cumulative events per day are compared to the cumulative events per second of the RXTE/ASM and Swift satellites [4].

The temporal (correlations between the variations in the X-ray and TeV bands) and the spectral (correlation of the spectral index with the TeV flux) analysis strongly support the predictions of the one-zone SSC model. A full account of this analysis can be found in [4].

3˙3. *MGRO J1908+06*. – The gamma-ray source MGRO J1908+06 was discovered by Milagro [6] at a median energy of ~ 20 TeV and recently associated with the Fermi pulsar 0FGL J1907.5+0602 [7]. HESS confirmed the discovery [8]. ARGO-YBJ observed a TeV emission from MGRO J1908+06 with a significance greater than 5 s.d. in a total on-source time of 5358 hours. The flux is $\sim$ 2-3 times larger than the flux quoted by HESS. MGRO J1908+06 is observed by ARGO-YBJ as a stable extended source ($\sigma = 0.49^\circ \pm 0.22^\circ$) with an integrated luminosity above 1 TeV ~ 1.8 times that of the Crab Nebula, making it one of the most luminous galactic gamma-ray source at TeV energies [9].

3˙4. *The Cygnus region*. – The Cygnus region has been studied by the ARGO-YBJ experiment by using data collected from November 2007 through August 2011 [10].

A TeV emission from a position consistent with TeV J2032+4130/MGRO J2031+41 is found with a significance of 6.4 s.d. The measured flux is much higher (about a factor 10) than the flux of TEV J2032+4130 as determined by HEGRA and MAGIC.

On the contrary, no evidence of a TeV emission above 3 s.d. is found at the location of MGRO J2019+37. At energies above 5 TeV the ARGO-YBJ exposure is still insufficient to reach a firm conclusion while at lower energies the ARGO-YBJ upper limit is marginally consistent with the spectrum determined by Milagro [12].

3˙5. *Diffuse emission from the Galactic Plane*. – Diffuse gamma-rays trace the location of the cosmic-ray sources and the distribution of interstellar gases. A very preliminary analysis of the events collected by ARGO-YBJ in about 4 years of data taking evidences a diffuse emission at energies > 300 GeV from the inner Galactic plane ($25^\circ < l < 85^\circ$, $|b| < 2^\circ$) with a measured flux $E^2 \cdot \mathrm{d}N/\mathrm{d}E = 1\text{–}1.5 \cdot 10^{-9}\,\mathrm{TeV\,cm^{-2}\,s^{-1}\,sr^{-1}}$ at 1 TeV, consistent with the predictions of the Fermi model of Galactic diffuse emission [11].

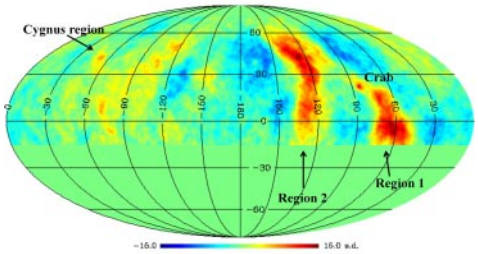

Fig. 2. – Medium scale CR anisotropy observed by ARGO-YBJ. The color scale gives the statistical significance of the observation in standard deviations.

3˙6. *Gamma-Ray Bursts.* – Working in scaler mode ARGO-YBJ has performed a search for high-energy emission from GRBs collecting data from November 2004 (corresponding to the Swift satellite launch) to April 2011, with a detector active area increasing from ~ 700 to $\sim 6700\,\mathrm{m}^2$. During this period, a total of 131 GRBs was inside the ARGO-YBJ field of view (*i.e.* with zenith angle $\theta \leq 45°$, limited only by atmospheric absorption); for 110 of these ARGO-YBJ data were available and they have been investigated by searching for a significant excess in the counting rates coincident with the satellite detection. No evidence of emission was found for any event. The fluence upper limits obtained in the 1–100 GeV energy range depend on the zenith angle, time duration and spectral index, reaching values down to $10^{-5}\,\mathrm{erg\,cm}^{-2}$. A detailed discussion on the methods and the first published results can be found in [13, 14].

4. – Cosmic-ray physics

4˙1. *Large and medium scale anisotropies.* – A large scale anisotropy at TeV energies is clearly observed by ARGO-YBJ with a significance greater than 20 s.d. Figure 2 shows the ARGO-YBJ sky map in equatorial coordinates after applying a high pass filter to evidence structures up to $\sim 35°$ wide. The most evident features are observed by ARGO-YBJ around the positions $\alpha \sim 120°$, $\delta \sim 40°$ and $\alpha \sim 60°$, $\delta \sim -5°$, positionally coincident with the regions detected by Milagro [15]. These regions, named "region 1" and "region 2", are observed with a statistical significance of about 14 s.d. On the left side of the sky map, several possible new extended features are visible, though less intense than those aforementioned. These structures could be related to the local magnetic field and source configuration, hence carrying key information on the origin of galactic cosmic rays.

4˙2. *Measurement of the light component spectrum of CRs.* – The ARGO-YBJ experiment is able to overlap direct measurements in a wide region below 100 TeV, not accessible by other extensive air shower experiments. The differential energy spectrum of the primary CR light component (p+He) has been measured by ARGO-YBJ in the energy region 5–250 TeV by using a Bayesian unfolding approach. The ARGO-YBJ data are fairly consistent with the values obtained by adding up the proton and helium fluxes measured by CREAM, concerning both the total intensities and the spectrum [16].

4˙3. *Measurement of the $\overline{p}/p$ ratio at TeV energies.* – In order to measure the $\overline{p}/p$ ratio at TeV energies we exploit the Earth-Moon system as an ion spectrometer: if protons are deflected towards East, antiprotons are deflected towards West.

The upper limits obtained by ARGO-YBJ are 5% at 1.4 TeV and 6% at 5 TeV assuming for the antiprotons the protons spectral index. In the few-TeV range the ARGO-YBJ

results are the lowest available, useful to constrain models for antiproton production in antimatter domains [17].

4˙4. *Measurement of the total p-p cross section.* – To make this measurement, the ARGO-YBJ data analysis is based on the study of the shower flux attenuation for different atmospheric depths. The Glauber theory has been used to infer the total proton-proton cross section σ_{pp}, up to a proton energy of 80 TeV, from the measured proton-air production cross section $\sigma_{p\text{-}air}$. The results favour the asymptotic $\ln^2(s)$ increase of total hadronic cross section [18]. The use of the analog RPC charge readout will allow to extend the study to collisions up to the PeV region.

5. – Interplanetary Magnetic Field measurement by Sun shadow

The same shadowing effect observed looking at cosmic rays in the direction of the Moon can be observed in the direction of the Sun, allowing the measurement of the transverse componet of the Interplanetary Magnetic Field (IMF). Using all data taken by the ARGO-YBJ from July 2006 to October 2009, the transverse component of the IMF, B_y, has been estimated at distances extending up to 0.5 A.U. with a minimal assumption on the model describing the IMF [19].

6. – Conclusions

The ARGO-YBJ detector is exploiting the performance of the RPCs to image the front of atmospheric showers with unprecedented resolution and detail. The digital and analog readout will allow a deep study of the CR phenomenology in the wide range from TeVs to PeVs. The results obtained in the low energy range after 3.5 years of data taking predict an excellent capability to address a wide range of important issues in Astroparticle Physics.

REFERENCES

[1] Aielli G. *et al.*, *Nucl. Instrum. Methods Phys. Res. A*, **562** (2006) 92.
[2] Bartoli B. *et al.*, *Phys. Rev. D*, **84** (2011) 022003.
[3] Aielli G. *et al.*, *Astrophys. J.*, **714** (2010) L208.
[4] Bartoli B. *et al.*, *Astrophys. J.*, **734** (2011) 110.
[5] Albert J. *et al.*, *Astrophys. J.*, **674** (2008) 1037.
[6] Abdo A. A. *et al.*, *Astrophys. J.*, **664** (2007) L91.
[7] Abdo A. A. *et al.*, *Astrophys. J.*, **700** (2009) L127.
[8] Aharonian F. *et al.*, *Astron. Astrophys.*, **499** (2009) 723.
[9] Bartoli B. *et al.*, *Astrophys. J.*, **760** (2012) 110.
[10] Bartoli B. *et al.*, *Astrophys. J.*, **745** (2012) L22.
[11] `http://fermi.gsfc.nasa.gov/ssc/data/access/lat/BackgroundModels.html`.
[12] Abdo A. A. *et al.*, 2012, arXiv:1202.0846.
[13] Aielli G. *et al.*, *Astrophys. J.*, **699** (2009) 1281.
[14] Aielli G. *et al.*, *Astropart. Phys.*, **32** (2009) 47.
[15] Abdo A. A. *et al.*, *Phys. Rev. Lett.*, **101** (2008) 221101.
[16] Bartoli B. *et al.*, *Phys. Rev. D*, **85** (2012) 092005.
[17] Bartoli B. *et al.*, *Phys. Rev. D*, **85** (2012) 022002.
[18] Aielli G. *et al.*, *Phys. Rev. D*, **80** (2009) 092004.
[19] Aielli G. *et al.*, *Astrophys. J.*, **729** (2011) 113.